

DEVELOPMENT AND EVALUATION OF A CONTINUUM NECK MUSCLE MODEL

AUTHORS:

Sofia Hedenstierna¹

Peter Halldin¹

Karin Brolin^{1,2}

¹ Royal Institute of Technology, Stockholm, Sweden

² Engineering Research Nordic AB, Linköping, Sweden

CORRESPONDENCE:

Sofia Hedenstierna

Neuronic Engineering, Royal Institute of Technology

Hälsövägen 7, 141 57 Huddinge

Phone +46 8 7904825

Fax +46 8 218368

Email sofia.hedenstierna@sth.kth.se

ABSTRACT

The Finite Element method is a powerful tool for analyzing the biomechanics of the human body. One area that has attracted increasing attention is the cervical musculature and its influence in neck injury mechanisms. Most cervical FE models of today use spring-elements as muscles and are limited to discrete geometries and nodal output results. A solid-element muscle model however, will improve the geometry and add properties such as tissue inertia and compressive stiffness. It also enables analysis of element stresses and strains within the muscular tissue. The aim of this study was to determine how a continuum muscle model influences the impact behavior of a human neck FE model compared to a discrete muscle model. The 3D geometries of the neck muscles were digitized from MR images of 50th percentile males and positioned relative to the KTH FE neck model in line with anatomical data from the literature. The muscles were modeled using solid finite elements and a non-linear, viscoelastic continuum material model. The behavior of the new muscle model during impact was compared to an existing discrete muscle model for frontal, rear-end, lateral and oblique impacts. The continuum muscle model stiffened the response of the KTH neck model and improved the boundary conditions for the vertebral column compared to a discrete model.

KEYWORDS:

Biomechanics, Muscle, FE modeling, non-linear, viscoelastic

INTRODUCTION

The Finite Element method, FEM, is a powerful tool in the study of the biomechanics of the human body. It is e.g. useful in the analysis of stresses and strains within biological tissues and injury mechanisms in complex systems such as the human neck. Most numerical models of the cervical spine of today include the cervical musculature [1, 2, 3, 4]. The majority use discrete elements, springs and dampers, to model the muscles whereas some models have developed a 3D musculature using shell or solid elements [4]. These 3D models include passive muscle properties and linear elastic materials or linear viscoelastic material models.

The discrete muscle models, DMM, including activation mainly use the Hill-type element, which consists of a contractile discrete element, elastic springs and viscous dampers. The total force (F_{tot}) is the sum of the contractile (F_{CE}) and the passive (F_{PE}) force contributions. In LS-Dyna [5] F_{PE} consists of an elastic spring and a viscous damper in parallel with the contractile force (F_{CE}), which's magnitude is dependant on muscle specific maximal isometric force (F_{max}); relative velocity of deformation (v_r); relative muscle length (l_r); and degree of activation over time (A):

$$F_{\text{CE}} = A(t) \cdot F_{\text{max}} \cdot f_V(v_r) \cdot f_L(l_r) \quad (\text{Eq. 1})$$

One Hill element usually represents a whole muscle consisting of identical sarcomeres and with a size ranging from a couple of mm to dm. This single element model gives adequate results in form of discrete nodal values of force and deflection for straight-line tension without interaction with surrounding tissues. However, it is less suitable for the study of complex musculoskeletal systems such as the neck, where the muscles cross over multiple joints and interact with surrounding tissues. It also does not allow for analysis of strain distributions within the muscles, which is of interest in the study of muscle injuries. On the other hand, this can be considered if using solid elements and continuum mechanical material descriptions instead of the discrete elements. Properties such as tissue inertia, compressive stiffness and friction between muscles will also be introduced into the model as well as an anatomically more correct geometry with curved force vectors.

The aim of this study was to develop a continuum FE muscle model as part of the KTH neck model, contributing with the above-mentioned properties and to evaluate how the continuum muscle model, CMM, influences the behavior of the KTH neck model compared to the existing DMM as well as how the strain distribution is predicted.

METHODS

The continuum muscle model was to be applied to an existing cervical column model known as the KTH neck model, Figure 1, which has been developed by the Department of Neuronic Engineering, KTH, Sweden [1,6], in the FE software of LS-DYNA [5]. The model has previously been validated both at motion segment level and as the entire cervical spine. For a more complete description and validation chart please refer to Brodin et al 2005 [1].

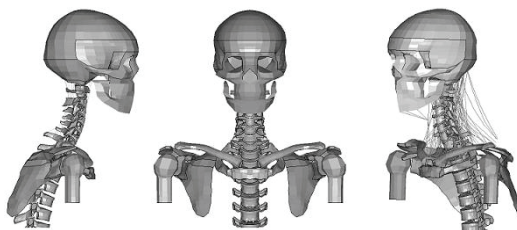


Figure 1 The KTH neck model including the rigid head and shoulder parts, to the right including the discrete cervical musculature elements

THE FE CERVICAL COLUMN MODEL

The model includes the seven cervical vertebrae with trabecular and compact bone tissue, the skull base, the facet joints with cartilage, the cervical ligaments, the intervertebral discs, and for boundary conditions a rigid skull and rigid shoulder parts. As a parallel part in the improvement of the KTH neck model the geometry of the vertebrae and particularly the facet joints has been refined. The same materials and source of geometry was used but with a refined mesh; resulting in more physiological correct motions of the vertebral joints.

THE DISCRETE MUSCLE MODEL

The KTH neck model also included a discrete element muscle model as seen to the right in Figure 1, consisting of Hill-type elements. The nodes of the discrete muscle elements were chosen according to anatomy literature [7]. To account for the neck curvature the superficial neck muscles that elongate over the complete cervical spine, e.g. the Trapezius and Splenius muscles were divided into two or more spring elements in series, with the nodes locked to the closest vertebra. The passive elastic material properties were defined with a bilinear curve approximated from the stress-strain curve of experiments on rabbit muscle performed by Myers et al [8], see Table 1. The active part of the muscle force was described by defining the muscle optimal length, peak force and

Physiological Cross Sectional Area (PCSA) for each muscle. Each muscle was also assigned a curve describing its activation as a function of time and load case [1].

Table 1 Material and element types for the muscles in the KTH neck model.

	Element type	Material type	Stiffness
Active Muscles DMM & CMM	2-node spring	Hill contractile	No passive stiffness
Passive Muscles DMM	2-node spring	Bilinear elastic, non-linear damper	0.5, 1.8 MPa #
Passive Muscles CMM	8-node solid	Ogden hyperelastic, linear viscoelasticity	$\mu_i=28643; 172000$ $\alpha_i=12; 0.5$ *

*Ogden parameters, # Passive stiffness below and above 12% strain.

THE CONTINUUM MUSCLE MODEL

The CMM introduced both a 3D geometry and continuum mechanical material properties to the model. The material and element description was evaluated for a mechanical test of a single rabbit muscle [9] before implemented in the FE model of the human neck.

MATERIAL AND ELEMENT DEFINITIONS

The approach for the CMM was to separate the active and passive parts of muscle force response to enable the use of commercially existing material models. Hence, the active part of the Hill elements were kept intact from the DMM and used in the CMM jointly with the solid elements.

The mechanical response of passive muscle tissue is similarly as for other biological soft tissues described by incompressibility, hyperelasticity and viscoelasticity. Hyperelastic materials are characterized by the strain energy potential that is non-dissipative, path independent and reversible. The viscoelastic material on the other hand includes a time and load rate dependency that consumes energy. These properties are also typical for rubber materials and the material model used for the passive muscle tissue was a rubber material defined by Ogden [10] also used in other models of muscle tissue. The material is described by the energy potential:

$$W = \sum_{i=1}^3 \sum_{j=1}^n \frac{\mu_j}{\alpha_j} (\lambda_i^{\alpha_j} - 1) + \frac{1}{2} K (J - 1)^2 \quad (\text{Eq. 2})$$

where K is the bulk modulus; J the Jacobian determinant; λ the principal stretches; and μ , α the Lamé constants. The hyperelastic material parameters were calculated by curve fitting to a tensile dynamic test on rabbit muscle [8]. The stress expression for uniaxial tensile stretch was derived from the strain energy as:

$$\sigma = \sum_i \mu_i \left(\lambda^{\alpha_i - 1} - \lambda^{-\frac{1}{2}\alpha_i - 1} \right). \quad (\text{Eq. 3})$$

The curve fitting method employed was the least square fit and the parameters were restricted to positive values to avoid numerical instabilities that were found in the implementation in LSDYNA. The viscoelasticity was implemented by adding a linear strain rate dependent stress component to the hyperelastic stress [5]. The time dependent shear modulus, $G(t)$, was described by a five term Prony series representing the relaxation curve of the material:

$$G(t) = \sum_{i=1}^n G_i e^{-\beta_i t} \quad (\text{Eq. 4})$$

MUSCLE GEOMETRY

The geometries of the muscles from skull to the 12th thoracic vertebrae were digitized from Magnetic Resonance Images, MRI, of 50th percentile male subjects.

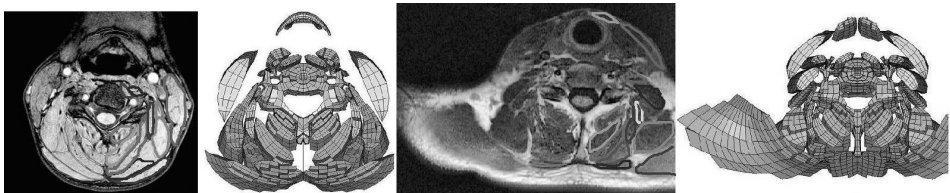


Figure 2 Segmented MR images of cervical muscles and approximate corresponding cross section from the meshed model.

The muscles were identified and segmented in the MRI, as seen in Figure 2, in accordance with anatomical guidebooks and morphometric literature [2,7,11]. Adjustments for a normal lordosis and element meshing were performed in the software Ropt – Rapid Optimization [12]. The muscles were modeled using solid eight node hexa-elements and six node wedge elements. At each end of the muscle a rigid end plate was defined and used in a rigid body attachment to the skeleton. The final model, seen in Figure 3, included 22 separate pairs of muscles that are listed in Table 2. The muscles

were compared with published data from cadaver studies concerning insertion points, length and mass [7, 11].

Table 2 Muscle mass and length as given by Goel et al [7], Kamibayashi and Richmond [11], and in the KTH neck model.

Muscles	Mass [g]			Length [mm]			No. of 2-node spring	PCSA ² cm ²
	[Goel]	[Kami]	KTH	[Goel]	[Kami]	KTH		
M. Rectus capitis post.majior	4.00	3.5	4.44	54.7		61		
M. Obliquus capitis superior	2.60	2.5	1.86	42		51	6	1.0
M. Obliquus capitis inferior	4.57	5.1	3.45	56.7	44	51		
M. Rectus capitis post minor	3.57	1	1.66	48.3		33	2	1.0
M. Interspinales							5	1.0
M. Semispinalis capitis	36.6	38.5	57.2	223	117	285	8 single and 8 multi**	8.6
M. Semispinalis cervicis	21.8		24.2	167		200		
M. Longissimus capitis	32.3		16.6	376		237	4 single 14multi**	2.5
M. Longissimus cervicis	32.5			268				
M. Iliocostalis cervicis			4.8			150		
M. Multifidus			55			440		
M. Splenius capitis	17.6	42.9	36.0	155	123	260	8 single 12multi**	4.5
M. Splenius cervicis	14.6		17.0	188	147	290		
M. Levator scapula	29.2		49	232	82	160	8 multi*	3.1
M. Trapezius	180	172.4	226	460	391	591	2 single 16multi**	13.7
M. Rectus capitis anterior			0.66			33		
M. Rectus capitis lateralis			1.1			29	4	0.9
M. Longus colli	6.87		10.5	103		188	17	1.4
M. Longus capitis	4.90	3.7	9.0	104	92	115	8	1.7
M. Scalenus anterior	7.67	5.6	8.4	91.3		115		
M. Scalenus medius	5.03	10.6	14.7	82.3		139	22	4.3
M. Scalenus posterior	8.47	10.8	6.9*	106		84*		
M. Sternocleidomastoideus	39.5	40.4	53.8	192	190	229	6 multi**	4.9
Infrahyoid			14.9			105	2	1.3
Suprahyoid							3	1.0

*Do not include the entire muscle, **Multi denotes a combination of two or more springs in series with intermediate nodes locked to a rigid vertebra, ²Physiological Cross Sectional Area as described in [1].

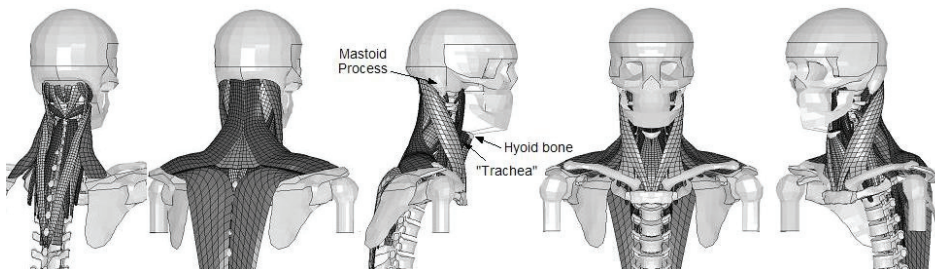


Figure 3 The KTH neck model with continuum element musculature.

KINEMATICAL VALIDATION AGAINST VOLUNTEER EXPERIMENTS

The KTH CMM model and the DMM were compared to published experimental sled tests on volunteers subjected to a frontal impact $-X$ acceleration of 15G [13] and volunteers subjected to a rearward impact $+X$ acceleration of 4G [14]. The simulations were performed both with and without activated Hill element musculature. The activation schemes used were the same for both models and developed for the DMM. The head kinematics of the two models was compared to that of the experiments.

STRAIN ANALYSIS

To examine how the continuum muscle model can be used to predict injury or fatigue in the muscle tissue the strain distribution and internal energy within the muscle elements were analyzed for the frontal and rear-end impact simulations.

RESULTS

The head kinematics from the frontal impact resulted in a head flexion with good validity for the first 180ms, Figure 4. After 180 ms the head of the volunteers stabilized itself while the model rebounded like an elastic spring. The difference between the spring and the CMM was small. Also the difference between the activated and the passive model was small.

Also for the rear-end impact the two models showed good correlation, Figure 5. There was a larger difference between the solid and DMM than for the frontal impact. Also the difference between active and passive models was greater.

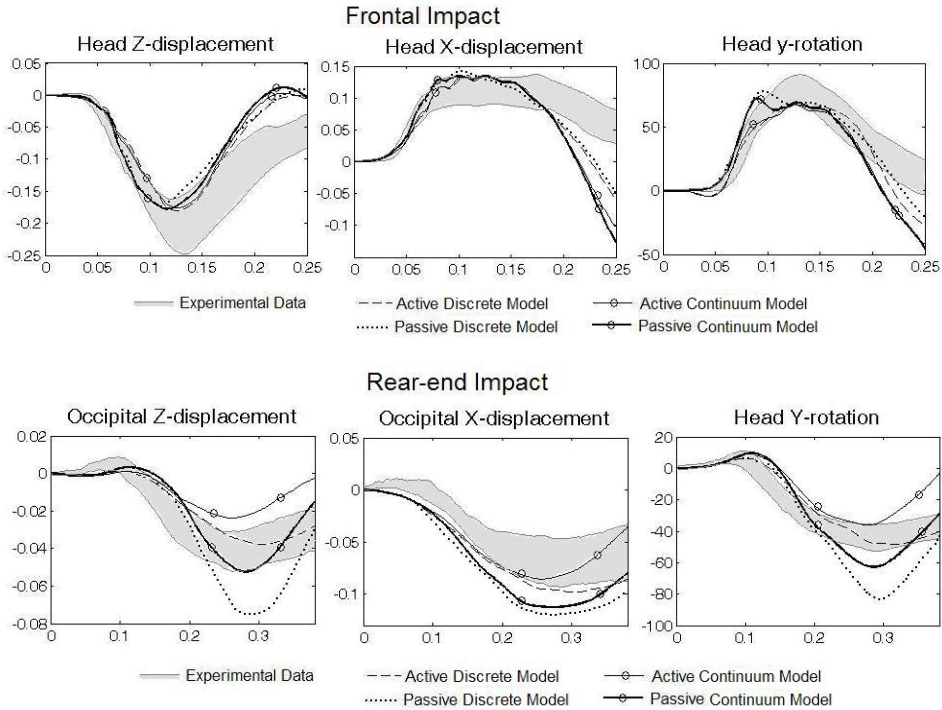


Figure 4 and Figure 5 Head relative T1 kinematics for the frontal and rear-end impact respectively for the solid and DMM in passive and active states together with the volunteer corridors.

STRAIN ANALYSIS

For the frontal impact the strains and energies were largest in the extensor muscles located posterior of the vertebral column, whereas for the rear-end impact high strains were found in the hyoid muscles which is the main flexor and in the suboccipital muscles, both posterior and anterior, Figure 6. Also the Splenius Capitis showed large strains. The highest strains were predicted at the time of maximal x-displacement for both impacts, Figure 7. Locally, the highest element strains were found at the insertion areas.

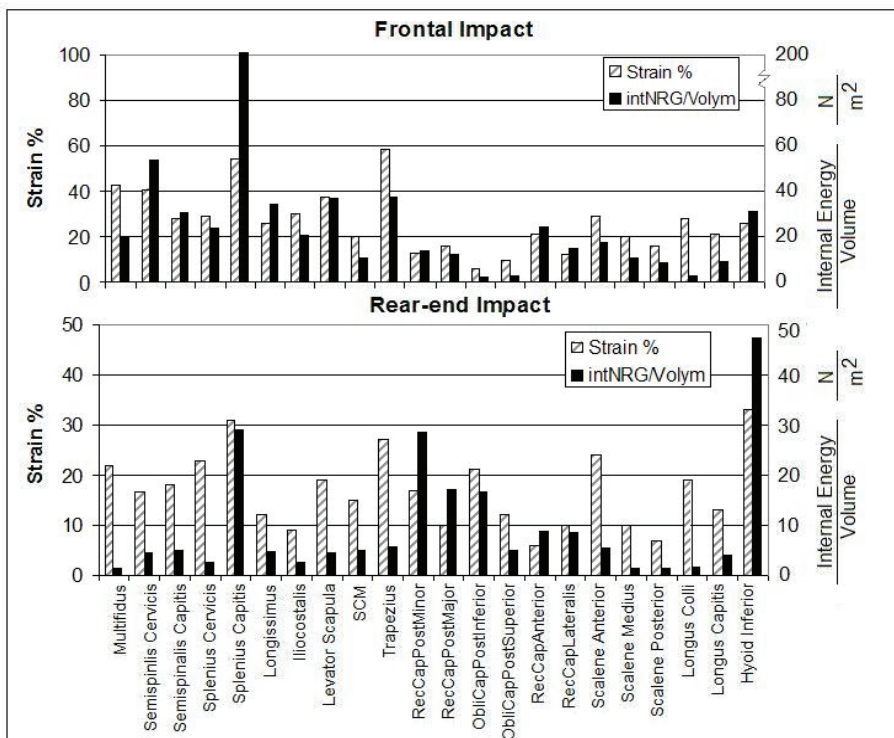


Figure 6 Maximal strain and maximal internal energy per muscle volume for each muscle during frontal and rear-end impact respectively.

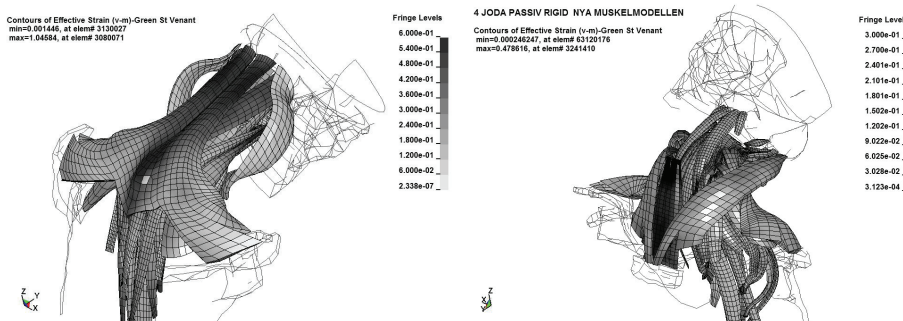


Figure 7 Posterior and Anterior view of the neck muscle model with visualized strains during frontal impact at t=98ms and during rear-end impact at t=285ms respectively.

DISCUSSION AND CONCLUSIONS

The continuum neck muscle model, CMM, has proven to work satisfactory for impact analysis in both flexion and extension. The head kinematics was similar to that of the DMM but the CMM behaved stiffer, especially in the rear-end low G impact. The main cause for this is probably the compressive resistance in the solid elements but could also appear due to inertial stiffness and contact friction between the muscles and their surrounding. The strain distribution mainly follows that of the internal energy except for very high strains at insertion points. These high strains arise since the model does not take the increasing stiffness in the myotendinous junctions into account, and can be excluded in a strain analysis. In the case of the rear-end impact some high compressive strains were found in the crease of buckling modes and are not reflected in the internal energy. The Ogden rubber parameter curve fit was performed for strain values below 30%. In the case of higher strains, it has been suggested [15] that initial tissue failure occurs in the muscle complex. Accordingly, the material parameters used overestimate the stiffness for strains above 30%. This is however compensated to some extent by the lack of stiff tendinous tissue surrounding the muscles. The Ogden rubber material model was chosen since it provided a better stress-strain curve fit than the other available hyperelastic materials. It also allows for the addition of separate compressive stiffness parameters in the future. The viscoelasticity in the model could be improved in the future by implementation of quasi-linear-elastic viscoelasticity.

The developed CMM is suitable for use in impact simulations of both low and intermediate acceleration pulses. The main benefits are the addition of strain distribution, geometrical flexibility, compressive properties, and contact interactions. The CMM is intended to be used when the continuum mechanical properties are of importance rather than the computer time.

REFERENCES

1. Brodin K, Halldin P, Leijonhufvud I., The Effect of Muscle Activation on Neck Response. *Traffic Injury Prevention* 6(1): 67-76, 2005.
2. Chancey VC, Nightingale RW, Van Ee CA., Improved Estimation of Human Neck Tensile Tolerances: Reducing the Range of Reported Tolerances Using Anthropometrically Correct Muscles and Optimized Physiological Loading. *Proceedings of the 47th Stapp Car Crash Conference*, 2003.
3. van der Horst M., Human Head Neck Response in Frontal, Lateral and Rear End Impact Loading. PhD thesis, Eindhoven Technische Universiteit, 2002.

4. Ejima S., Ono K., Kaneoka K., Fukushima M. Development and validation of the human neck muscle model under impact loading. IRCOBI conference proceeding, 2005.
5. Hallquist, J. O., LS-DYNA. Keyword User's Manual. Version 971, Livermore Software Technology Corporation, Livermore, 2007.
6. Halldin P. Prevention and prediction of head and neck injury in traffic accidents - using experimental and numerical methods. PhD thesis, Royal Institute of Technology, Stockholm, Sweden, 2001.
7. Goel VK., Liu Y., Clark CR. Quantitative Geometry of the Muscular Origins and Insertions of the Human Head and Neck, Mechanisms of Head and Spine Trauma, Chapter 13, Pages 397-415, Aloray Publisher, 1986.
8. Myers B., Van Ee C., Camacho DLA., Woolley CT., Best TM. On the Structural and Material Properties of Mammalian Skeletal Muscle and Its Relevance to Human Cervical Impact Dynamics. Proceedings of the 39th Stapp Car Crash Conference 1995.
9. Hedenstierna S., Halldin P., Brodin K., Evaluation of a combination of continuum and discrete finite elements in a model of passive and active muscle tissue. Submitted to Computer Methods in Biomechanics and Biomedical Engineering, 2007.
10. Ogden R.W. Large Deformation Isotropic Elasticity: On the Correlation of Theory and Experiment for Compressible Rubber like Solids. Proc.R.Soc. Lond. A. 38, 567-583, 1972.
11. Kamibayashi L., Richmond F., Morphometry of Human Neck Muscles. Spine, 23, pp1314-1323, 1998.
12. Alfgam Optimering AB, S-135 48 TYRESÖ, www.alfgam.se, 29/03/2007
13. Ewing CL., Thomas DJ., Lustick L. The effect of duration, rate of onset and peak sled acceleration on the dynamic response of the human head and neck. Proceedings of the 20th Stapp Car Crash Conference, pp. 3-41, 1976.
14. Davidsson Johan, Development of a Mechanical Model for Rear Impacts. PhD Thesis, Chalmers Technical University, Gothenburg, Sweden. 2000.
15. Best T.M., A Biomechanical Study of Skeletal Muscle Strain Injuries. PhD thesis, Department of Biomedical Engineering, Duke University, 1993.

